Polymer Journal (2017) 49, 735–739

www.nature.com/pj

ORIGINAL ARTICLE

Macromolecular templates for biomineralization-inspired crystallization of oriented layered zinc hydroxides

Fumiya Katase, Satoshi Kajiyama and Takashi Kato

Biomineralization-inspired approaches are environmentally friendly processes for developing organic/inorganic hybrids with ordered structures. This study demonstrates a biomineralization-inspired approach that is expanded to form organic/inorganic hybrid thin films based on a zinc-layered compound with an organic molecule. The interactions between the acidic polymers and the zinc ions transiently inhibit crystallization in solution, thereby inducing crystallization on/in the insoluble polymer templates. In addition, poly(vinyl alcohol) provides a template for the specific crystallographic orientation of the zinc-layered compounds. The cooperative effects of the soluble and insoluble macromolecular templates lead to the structural and orientational control of organic/inorganic hybrids based on a zinc-layered compound with an organic molecule.
Polymer Journal (2017) **49,** 735–739; doi:10.1038/pj.2017.42; published online 9 August 2017

INTRODUCTION

Living organisms elaborate well-defined organic/inorganic composites via biomineralization processes.[1–5] Biomineralization is an attractive model for environmentally friendly processing to develop functional materials with well-defined ordered structures.[6–24] In the biomineralization process, insoluble macromolecular templates play crucial roles with soluble biopolymers to control the nanostructures and crystallographic orientation of the inorganic components. Inspired by biomineralization, insoluble solid templates have been utilized to develop ordered nanohybrid structures based on calcium carbonate ($CaCO_3$)[6–14] and calcium phosphate[15–20] as well as transition metal compounds.[21–24] Macromolecular templates can accommodate functional organic molecules with ordered organic/inorganic hybrids.[25] Alignment control of organic molecules has not been sufficiently achieved, even though a few examples of crystallization control of organic compounds through biomineralization-inspired approaches have been reported.[26,27]

Poly(vinyl alcohol) (PVA) is a useful matrix for the crystallization of the inorganic crystals. The local crystalline structures of PVA that are formed through hydrogen bonds between −OH groups provide effective templates. For example, the PVA crystalline structure induces the formation of the aragonite phase for $CaCO_3$.[28–31] Moreover, we have demonstrated that PVA thin-film matrices can serve as templates for strontium carbonate,[32] octacalcium phosphate[33] and zinc carbonate hydroxides[34] with ordered structures.

Here, our aim is to use PVA templates to develop ordered organic/inorganic hybrids based on layered inorganic compounds (Figure 1). Inorganic layered compounds can accommodate organic molecules in their interlayer space due to weak van der Waals interactions in their layers.[35–47] Intercalating layered compounds are of broad interest in materials science due to the functional properties of inorganic compounds and organic phases.[35–40] Their orientation control is a challenging issue for tuning their functions. Oriented structures in organic/inorganic nanohybrid materials based on intercalating layered compounds have been obtained using the hydrothermal reaction[48–50] or electrodeposition on conductive substrates.[51,52] However, no biomineralization-inspired approach for the formation and structural control of hybrid thin films consisting of intercalating layered compounds under ambient conditions has been attempted.

In the present study, we have used thin-film macromolecular templates of PVA for orientational control of the layered zinc hydroxide compounds with an organic molecule (that is, 4-ethoxybenzoic acid (BA)) (Figure 1). This organic compound was used to induce the formation of sheet-like crystals with a large interlayer space for the zinc-layered compounds. This morphological control of the zinc compound crystals is key for topotactic conversion to ZnO with thermal treatment.[53,54] The intercalation of the rigid molecule may suppress the aggregation of ZnO particles across the layer structure. The formation of hybrid thin films could be achieved through the cooperative effects of the soluble and insoluble polymers.

EXPERIMENTAL PROCEDURES

Materials

Zinc nitrate hexahydrate ($Zn(NO_3)_2{\cdot}6H_2O$, 99.9%) was purchased from Wako Pure Chemical Industries, Ltd (Osaka, Japan). PVA (Average $M_W = 1.46 \times 10^5$ to 1.86×10^5, 87–89% hydrolyzed), poly(acrylic acid) (PAA, $M_W = 1.8 \times 10^3$) and sodium hydroxide (NaOH) (97%) were purchased from Sigma-Aldrich (St Louis, MO, USA). BA (98.0%) was purchased from Tokyo Chemical

Department of Chemistry and Biotechnology, School of Engineering, The University of Tokyo, Tokyo, Japan
Correspondence: Professor T Kato, Department of Chemistry and Biotechnology, School of Engineering, The University of Tokyo, 7-3-1 Hongo, Bunkyo-ku, Tokyo 113-8656, Japan.
E-mail: kato@chiral.t.u-tokyo.ac.jp
Received 25 May 2017; revised 20 June 2017; accepted 21 June 2017; published online 9 August 2017

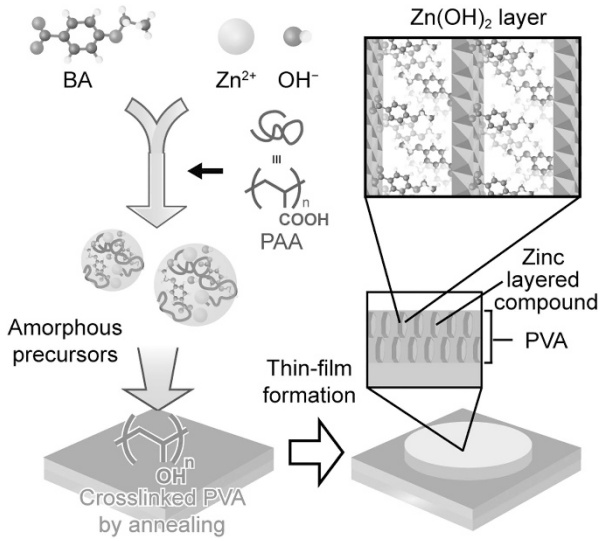

Figure 1 Schematic illustration of the strategy for biomineralization-inspired thin-film formation consisting of layered zinc hydroxides intercalating 4-ethoxybenzoic acid (BA) on thin-film macromolecular templates. A full color version of this figure is available at *Polymer Journal* online.

Industry Co., Ltd (Tokyo, Japan). All chemical reagents were used without further purification.

Preparation of PVA templates

PVA was dissolved in dimethyl sulfoxide (DMSO) at a concentration of 4.0 wt%. The DMSO solution of PVA was spin-coated on glass substrates followed by annealing at 200 °C for 30 or 60 min under ambient conditions.

Precipitation experiments of zinc-layered compounds

Precipitates of layered zinc hydroxides were obtained using a precipitation method. The precursor solution of BA (40 mM) was prepared with an aqueous NaOH solution (100 mM). The BA solution was mixed with an equal volume of an aqueous $Zn(NO_3)_2{\cdot}6H_2O$ solution (40 mM). The mixed solution was placed in an incubator, which maintained the reaction temperature at 40 °C for 3 days. The resulting precipitates were collected by centrifugation and washed with purified water. To obtain the precipitates formed in the presence of PAA, PAA was dissolved in the $Zn(NO_3)_2{\cdot}6H_2O$ solution (40 mM) at a concentration of 2.2×10^{-1} wt% prior to mixing the two precursor solutions.

Preparation of thin-film hybrids composed of layered zinc hydroxides and PVA

The PVA templates on glass substrates were immersed into the crystallization solution. The final concentrations of BA, NaOH, $Zn(NO_3)_2{\cdot}6H_2O$, and PAA in the crystallization solution were adjusted to 20, 50 and 20 mM, and 1.1×10^{-1} wt%, respectively. The temperature was maintained at 40 °C during the crystallization. After 3 days, the thin-film hybrids were washed with purified water and dried at room temperature.

Characterization

The morphologies were observed using scanning electron microscopy (SEM) (Hitachi High-Technologies, Tokyo, Japan, S-4700, operated at 3.0 kV). A platinum coating was performed as a conductive treatment with a Hitachi E-1030 ion sputter. The X-ray diffraction (XRD) patterns were recorded with a SmartLab X-ray diffractometer (Rigaku, Tokyo, Japan) using a paralleling beam method with CuKα radiation ($\lambda = 0.154$ nm). The XRD measurements for the thin-film hybrids were conducted in two types of geometries (that is, out-of-plane with 2θ scanning and in-plane with $2\theta\chi$ scanning). The Fourier transform infrared (FTIR) spectra were recorded using the KBr method with a JASCO/FTIR-6100 spectrometer. Thermogravimetric (TG) analyses were performed with a TG-8120 (Rigaku, Tokyo, Japan) under an air flow up to 1000 °C at a heating rate of 10 °C min^{-1}.

RESULTS AND DISCUSSION

The insoluble PVA templates were prepared by spin-coating the DMSO solution containing PVA, followed by an annealing process at 200 °C to crosslink the main chains.[30] Two types of PVA templates, which were annealed for 30 min (template I) and 60 min (template II) at 200 °C, were used as matrices for the zinc-layered compounds. The solutions for crystallization were prepared by mixing equal volumes of an aqueous solution containing $Zn(NO_3)_2{\cdot}6H_2O$ (40 mM) and PAA (2.2×10^{-1} wt%) as the soluble polymer and an aqueous solution containing BA (40 mM) and NaOH (100 mM). The insoluble PVA templates were placed into the crystallization solution for 3 days at 40 °C to achieve thin-film formation of zinc hydroxides intercalating BA (Zn/BA). After being washed with deionized water, the Zn/BA hybrid thin films were obtained.

The SEM observation of the thin films (Figure 2) indicates that the morphologies are changed by the annealing time of the PVA matrices as well as the $CaCO_3$ system.[30,31] When template I was used, spherulitic thin films with a domain size of a few micrometers were formed after crystallization (Figure 2a, left). The thickness of the spherulitic thin films was estimated to be 800 nm based on the cross-sectional SEM observation (Figure 2a, right). The cross-sectional SEM observation also indicated that crystallization occurs from the inside of the PVA matrix (Figure 2a, right). In contrast, hybrid thin films with the thickness of 5 μm were formed on template II (Figure 2b). Although the thicknesses of templates I and II are similar (Supplementary Figure S1), the thicknesses of the Zn/BA thin films were largely different in the SEM observation. The difference in the thicknesses of the hybrid thin films was caused by the crystallization site. For template II, the crystallization of the Zn/BA thin films starts at the surface of template II, and then, the Zn/BA crystals grow to the solution side, as shown in Figure 2b, right. The crystal growth on the solution side induces thicker film formation than that on the hydrogel thin-film template due to the absence of the spatial restriction.

The effects of the annealing process on the properties of the PVA templates have been examined using FTIR and TG measurements. In

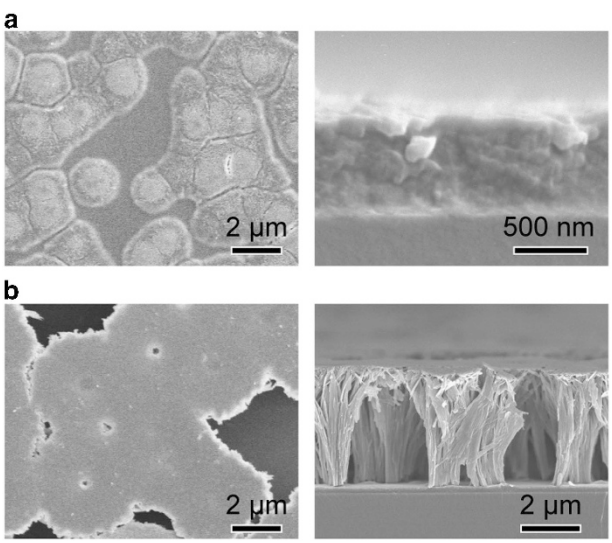

Figure 2 SEM images of thin films composed of Zn/BA and PVA matrices. Top-view (left) and cross-sectional view (right) of the hybrid thin films formed with (**a**) template I and (**b**) template II. BA, 4-ethoxybenzoic acid; PVA, poly(vinyl alcohol); SEM, scanning electron microscopy.

the FTIR measurements, the broad peak corresponding to OH stretching between 3000 and 3700 cm^{-1} shifts to a higher wavenumber as the annealing time increased (Supplementary Figure S2). The shoulder peak at 1082 cm^{-1} attributed to the backbone stretching of ether bonds was observed in the FTIR spectrum for the PVA annealed for 120 min. These results suggest that the annealing process at 200 °C enhances the hydrogen bonding between the OH groups and induces the dehydration reaction between the OH groups.[55] TG analyses for the DMSO solution containing PVA also support a dehydration reaction in PVA during the annealing process (Supplementary Figure S3). The gradual weight loss after DMSO evaporation was due to the dehydration reaction of PVA. The dehydration degree affects the ion accommodating ability of the PVA hydrogel templates. Therefore, for template II, Zn/BA crystallization occurs on the surface of the matrix due to the low accessibility for ions.

To evaluate the crystallographic orientation of the hybrid thin films, the XRD patterns of the hybrid thin films were measured in two different geometries (that is, out-of-plane with 2θ scanning and in-plane with $2\theta\chi$ scanning) (Figure 3). In general, intercalating layered zinc compounds exhibit harmonic diffraction of the 00*l* peaks due to the interlayer space at the lower-angle region, and two peaks corresponding to the 100 and 110 reflections were due to the intralayer structure.[37,51,52] Only two peaks due to the 100 and 110 reflections were observed at 33 and 59° in the out-of-plane XRD pattern of the thin film (Figure 3a). However, the peaks corresponding to the 00*l*, 100 and 110 reflections were observed in the in-plane XRD pattern (Figure 3b). These results suggest that the hybrid thin films that formed with template I exhibit the specific oriented structure where the zinc hydroxide layers are aligned perpendicular to the substrate. The oriented structure is similar to the zinc hydroxide carbonate/PVA hybrid thin films prepared through a biomineralization-inspired approach in our previous study.[34] As was previously reported, the hydrophilic conditions inside the PVA template induces the perpendicular orientation of the zinc hydroxide layers.[34,56] For the hybrids with template II, the 00*l*, 100 and 110 reflections were observed in both in-plane and out-of-plane XRD patterns, suggesting the random crystallographic orientation of the hybrid thin films. The random crystallographic orientation was induced by template II because thin films are formed on the surface

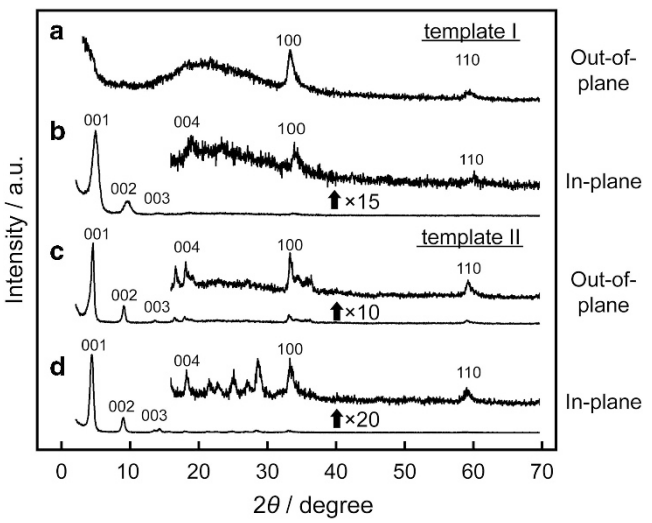

Figure 3 (**a**, **c**) Out-of-plane and (**b**, **d**) in-plane XRD patterns of the hybrid thin films formed with (**a**, **b**) template I and (**c**, **d**) template II. The scan rate was 0.2° min^{-1}. XRD, X-ray diffraction.

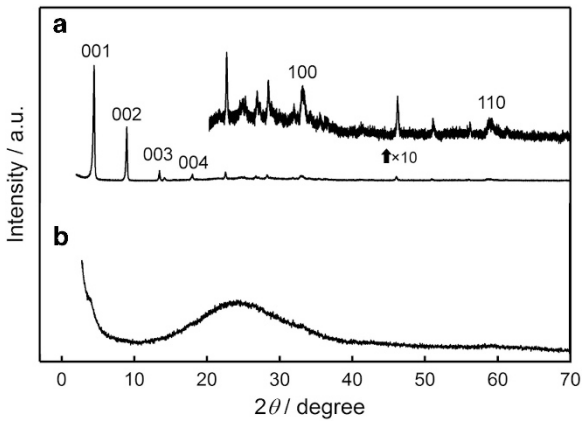

Figure 4 XRD patterns of the precipitates formed without PVA templates: (**a**) in the absence of PAA and (**b**) in the presence of PAA. PAA, poly(acrylic acid); PVA, poly(vinyl alcohol); XRD, X-ray diffraction.

of template II where the PVA template has a smaller effect on the crystallization. Peaks other than the 00*l*, 100 and 110 reflections are observed in the XRD pattern of the hybrid with template II (Figures 3c and d). Although the detailed crystal structure remains unclear, these peaks suggest the high crystallinity of Zn/BA, which was formed with the PVA matrices in the presence of PAA. These peaks are most likely caused by the superstructure due to the arrangement of intercalated anions and water molecules similar to that observed in other layered double hydroxides.[57] The crystal growth on the surface of template II also induced the high crystallinity due to fast ion diffusion in the solution compared to that inside of the hydrogel templates.

For the thin-film formation of Zn/BA with the PVA templates, the PAA soluble polymer played a crucial role based on a comparison of the precipitates prepared in the absence and presence of 1.1×10^{-1} wt% PAA. The XRD pattern (Figure 4a) suggests the high crystallinity of the precipitates in the absence of the soluble polymer (PAA). The interlayer distance was estimated to be 19.8 Å, which is the same as that in the Zn/BA crystals with the templates. In this case, the Zn/BA crystals were immediately formed in the solution. In the presence of PAA, colloidal particles were formed. The resulting powder, which was obtained by centrifugation of the colloidal particles and vacuum dried, did not exhibit a crystalline structure (Figure 4b). The TG and FTIR measurements suggest that the colloidal particles include PAA (Figure 5). Zn/BA crystals exhibit three weight loss steps in the TG measurement up to 1000 °C under an air flow as follows: (i) evaporation of intercalated water molecules at 100 °C, (ii) dehydration of hydroxide groups in the inorganic layers at 180 °C and (iii) decomposition of organic components at 400 °C (Figure 5a). After the decomposition of the organic components, Zn/BA was eventually converted to ZnO.[58] In the presence of PAA, the weight loss at 180 °C decreases but the weight loss at 400 °C increases compared to the Zn/BA precipitate without PAA. These results suggest that hydroxide anions partially exchange with PAA, which interacts with the zinc ions through the carboxyl groups. The FTIR measurements suggest the coordination of BA and PAA to zinc ions (Figure 5b). In the absence of PAA, two peaks were observed at 1545 and 1420 cm^{-1} (Figure 5b, bottom), which were due to the C=O stretching of the monodentate coordination of the carboxylate to the zinc ions.[59] In the presence of PAA, the FTIR spectrum contains broad peaks at 1700, 1550 and 1420 cm^{-1} due to C=O stretching (Figure 5b, middle), suggesting the random coordination of carboxyl groups to zinc ions due to the amorphous structure of the colloidal particles. In the absence of PAA,

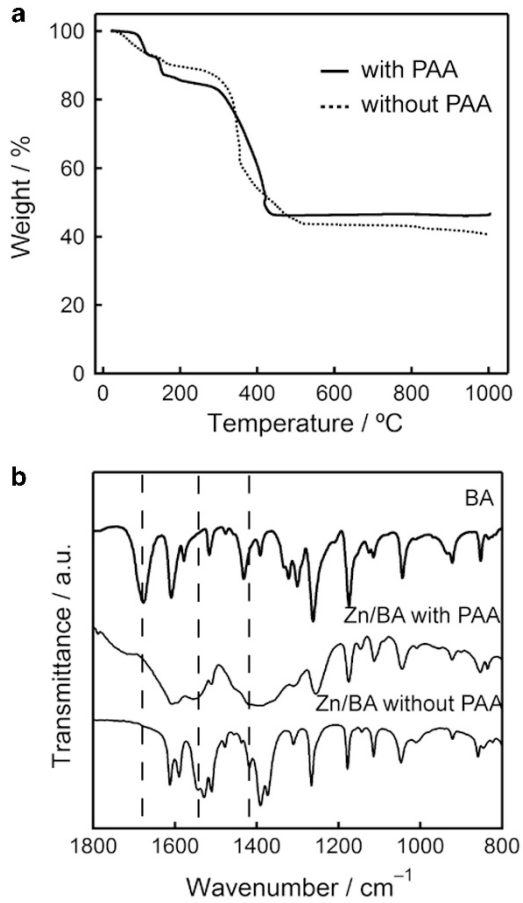

Figure 5 (**a**) TG curves of Zn/BA precipitates obtained in the presence (solid line) and absence (dotted line) of PAA (heating rate:10 °C min^{-1}) (**b**) FTIR spectra of BA crystal and Zn/BA precipitated in the presence and absence of PAA using the KBr method. BA, 4-ethoxybenzoic acid; FTIR, Fourier transform infrared; PAA, poly(acrylic acid); TG, thermogravimetric.

rectangular-shaped crystals were observed on the surface of both templates I and II using SEM (Supplementary Figure S4). Therefore, PAA serves as an inhibitor of immediate crystallization in solution by the coordination to zinc ions. The transient inhibition of the crystallization is important for the formation of organic/inorganic hybrids with insoluble macromolecular templates because it enables resource ions to reach the surface or inside of the templates prior to crystallization.

It is important to note that the colloidal particles that were formed in the presence of PAA did not crystallize within 3 days at 40 °C on the solution side. However, the crystallization occurred inside the PVA matrix, suggesting that the PVA matrices induce the crystallization of Zn/BA. The cooperative interactions between PAA and PVA are necessary for the formation of spherulitic hybrid thin films. The inhibition of sudden crystallization in solution and the combination of soluble polymer additives and insoluble polymer matrices are important for controlling the ordered structures in these intercalating hybrid thin films using the approach inspired by biomineralization.

The present study demonstrates the formation of hybrid structures composed of layered zinc hydroxides and macromolecular templates under mild conditions. The nanostructures of the organic/inorganic hybrid thin films could improve the properties of zinc oxides (for example, photocatalytic properties).[34,60] Environmentally friendly processes inspired by biomineralization using macromolecular templates have been applied for structural control of minerals that cannot be found in nature, leading to the development of highly functional materials.

CONCLUSIONS

In summary, we have successfully prepared hybrid thin films of Zn/BA-layered compounds with macromolecular templates consisting of crosslinked PVA using an approach inspired by biomineralization under mild conditions. The obtained hybrid thin films exhibit specific crystallographic orientation, which will be important for further functionalization. The ordered structures of the Zn/BA-layered compounds depend on the annealing time of the thin-film PVA templates, which changes the hydrophilicity of the templates. This study demonstrates that biomineralization-inspired approaches can be expanded for the orientational control of layered compounds with organic molecules. Further design of target materials and macromolecular templates will lead to the development of novel functional materials prepared under mild conditions.

CONFLICT OF INTEREST

The authors declare no conflict of interest.

ACKNOWLEDGEMENTS

This study was partially supported by JSPS KAKENHI Grant No JP15H02179.

1 Bäuerlein, E., Behrens, P. & Epple, M. *Handbook of Biomineralization* (Wiley-VCH, Weinheim, Germany, 2007).
2 Cantaert, B., Kuo, D., Matsumura, S., Nishimura, T., Sakamoto, T. & Kato, T. Use of amorphous calcium carbonate for the design of new materials. *ChemPlusChem.* **82**, 107–120 (2017).
3 Vidavsky, N., Addadi, S., Mahamid, J., Shimoni, E., Ben-Erza, D., Shpigel, M., Weiner, S. & Addadi, L. Initial stages of calcium uptake and mineral deposition in sea urchin embryos. *Proc. Natl Acad. Sci. USA* **111**, 39–44 (2014).
4 Grunenfelder, L. K., Herrera, S. & Kisailus, D. Crustacean-derived biomimetic components and nanostructured composites. *Small* **10**, 3207–3232 (2014).
5 Arakaki, A., Shimizu, K., Oda, M., Sakamoto, T., Nishimura, T. & Kato, T. Biomineralization-inspired synthesis of functional organic/inorganic hybrid materials: organic molecular control of self-organization of hybrids. *Org. Biomol. Chem.* **13**, 974–989 (2015).
6 Nishimura, T. Macromolecular templates for the development of organic/inorganic hybrid materials. *Polym. J.* **47**, 235–243 (2015).
7 Finnemore, A., Cunha, P., Shean, T., Vignolini, S., Guldin, S., Oyen, M. & Steiner, U. Biomimetic layer-by-layer assembly of artificial nacre. *Nat. Commun.* **3**, 966 (2012).
8 Yamamoto, Y., Nishimura, T., Saito, T. & Kato, T. $CaCO_3$/chitin-whisker hybrids: formation of $CaCO_3$ crystals in chitin-based liquid-crystalline suspension. *Polym. J.* **42**, 583–586 (2010).
9 Matsumura, S., Kajiyama, S., Nishimura, T. & Kato, T. Formation of helically structured chitin/$CaCO_3$ hybrids through an approach inspired by the biomineralization processes of crustacean cuticles. *Small* **11**, 5127–5133 (2015).
10 Nakayama, M., Kajiyama, S., Nishimura, T. & Kato, T. Liquid-crystalline calcium carbonate: biomimetic synthesis and alignment of nanorod calcite. *Chem. Sci.* **6**, 6230–6234 (2015).
11 Mao, L.-B., Gao, H.-L., Yao, H.-B., Liu, L., Cölfen, H., Liu, G., Chen, S.-M., Li, S.-K., Yan, Y.-X., Liu, Y.-Y. & Yu, S.-H. Synthetic nacre by predesigned matrix-directed mineralization. *Science* **354**, 107–110 (2016).
12 Nishio, T., Tanaka, Y. & Naka, K. Preparation of composites of liquid-crystalline matrix of poly(*p*-phenylene-sulfoterephtalamide) and $CaCO_3$ by *in situ* mineralization. *J. Appl. Polym. Sci.* **132**, 41455 (2015).
13 Tajima, T., Tsutsui, A., Fujii, T., Takada, J. & Takaguchi, Y. Fabrication of novel core-shell microspheres consisting of single-walled carbon nanotubes and $CaCO_3$ through biomimetic mineralization. *Polym. J.* **44**, 620–624 (2012).
14 Cantaert, B., Kim, Y.-Y., Ludwig, H., Nudelman, F., Sommerdijk, N. A. J. M. & Meldrum, F. C. Think positive: phase separation enables a positively charged additive to induce dramatic changes in calcium carbonate morphology. *Adv. Funct. Mater.* **22**, 907–915 (2012).
15 Nudelman, F., Pieterse, K., George, A., Bomans, P. H. H., Friedrich, H., Brylka, L. J. & Hilbers, P. A. J. de With, G. & Sommerdijk, N. A. J. M. The role of collagen in bone apatite formation in the presence of hydroxyapatite nucleation inhibitors. *Nat. Mater.* **9**, 1004–1009 (2010).

16 Ogiwara, T., Katsumura, A., Sugimura, K., Teramoto, Y. & Nishio, Y. Calcium phosphate mineralization in cellulose derivative/poly(acrylic acid) composites having a chiral nematic mesomorphic structure. *Biomacromolecules* **16**, 3959–3969 (2015).
17 Morimune-Moriya, S., Kondo, S., Sugawara-Narutaki, A., Nishimura, T., Kato, T. & Ohtsuki, C. Hydroxyapatite formation on oxidized cellulose nanofibers in a solution mimicking body fluid. *Polym. J.* **47**, 158–163 (2015).
18 Takeoka, Y., Hayashi, M., Sugiyama, N., Yoshizawa-Fujita, M., Aizawa, M. & Rikukawa, M. *In situ* preparation of poly(L-lactic acid-*co*-glycolic acid)/hydroxyapatite composites as artificial bone materials. *Polym. J.* **47**, 164–170 (2015).
19 Iijima, K., Nagahama, H., Takada, A., Sawada, T., Serizawa, T. & Hashizume, M. Surface functionalization of polymer substrates with hydroxyapatite using polymer-binding peptides. *J. Mater. Chem. B* **4**, 3651–3659 (2016).
20 Nakamura, K., Oaki, Y. & Imai, H. Multistep crystal growth of oriented fluorapatite nanorod arrays for fabrication of enamel-like architectures on a polymer sheet. *CrystEngComm.* **19**, 669–674 (2017).
21 Dang, F., Hoshino, T., Oaki, Y., Hosono, E., Zhou, H. & Imai, H. Synthesis of Li-Mn-O mesocrystals with controlled crystal phases through topotactic transformation of $MnCO_3$. *Nanoscale* **5**, 2532–2537 (2013).
22 Kajiyama, S., Kumagai, H., Nishimura, T. & Kato, T. Formation of rectangular plate-like α-MnOOH and sheet-like γ-MnOOH by slow diffusion of ammonia vapor. *Chem. Lett.* **42**, 341–343 (2013).
23 Asenath-Smith, E., Hovden, R., Kourkoutis, L. F. & Estroff, L. A. Hierarchically structured hematite architectures achieved by growth in a silica hydrogel. *J. Am. Chem. Soc.* **137**, 5184–5192 (2015).
24 Lenders, J. J. M., Zope, H. R., Yamagishi, A., Bomans, P. H. H., Arakaki, A., Kros, A., de With, G. & Sommerdijk, N. A. J. M. Bioinspired magnetite crystallization directed by random copolypeptides. *Adv. Funct. Mater.* **25**, 711–719 (2015).
25 Zhu, F., Nishimura, T. & Kato, T. Organic/inorganic fusion materials: cyclodextrin-based polymer/$CaCO_3$ hybrids incorporating dye molecules through host-guest interactions. *Polym. J.* **47**, 122–127 (2015).
26 Huang, M., Schilde, U., Kumke, M., Antonietti, M. & Cölfen, H. Polymer-induced self-assembly of small organic molecules into ultralong microbelts with electronic conductivity. *J. Am. Chem. Soc.* **132**, 3700–3707 (2010).
27 Okaniwa, M., Oaki, Y. & Imai, H. Morphology and orientation control of organic crystals in organic media through advanced biomimetic approach. *Bull. Chem. Soc. Jpn* **88**, 1459–1465 (2015).
28 Hosoda, N., Sugawara, A. & Kato, T. Template effect of crystalline poly(vinyl alcohol) for selective formation of aragonite and vaterite $CaCO_3$ thin films. *Macromolecules* **36**, 6449–6452 (2003).
29 Kim, I. W., Robertson, R. E. & Zand, R. Effects of some nonionic polymeric additives on the crystallization of calcium carbonate. *Cryst. Growth Des.* **5**, 513–522 (2005).
30 Sakamoto, T., Oichi, A., Nishimura, T., Sugawara, A. & Kato, T. Calcium carbonate/polymer thin-film hybrids: induction of the formation of patterned aragonite crystals by thermal treatment of a polymer matrix. *Polym. J.* **41**, 522–523 (2009).
31 Kajiyama, S., Nishimura, T., Sakamoto, T. & Kato, T. Aragonite nanorods in calcium carbonate/polymer hybrids formed through self-organization processes from amorphous calcium carbonate solution. *Small* **10**, 1634–1641 (2014).
32 Sakamoto, T., Nishimura, Y. & Kato, T. Tuning of morphology and polymorphs of carbonate/polymer hybrids using photoreactive polymer templates. *CrystEngComm.* **17**, 6947–6954 (2015).
33 Kajiyama, S., Sakamoto, T., Inoue, M., Nishimura, T., Yokoi, T., Ohtsuki, C. & Kato, T. Rapid and topotactic transformation from octacalcium phosphate to hydroxyapatite (HAP): a new approach to self-organization of free-standing thin-film HAP-based nanohybrids. *CrystEngComm.* **18**, 8388–8395 (2016).
34 Matsumura, S., Horiguchi, Y., Nishimura, T., Sakai, H. & Kato, T. Biomineralization-inspired preparation of zinc hydroxide carbonate/polymer hybrids and their conversion into zinc oxide thin-film photocatalysts. *Chem. Eur. J.* **22**, 7094–7101 (2016).
35 Ruiz-Hitzky, E. Conducting polymers intercalated in layered solids. *Adv. Mater.* **5**, 334–340 (1993).
36 Ogawa, M. & Kuroda, K. Photofunctions of intercalation compounds. *Chem. Rev.* **95**, 399–438 (1995).
37 Sofos, M., Goldberger, J., Stone, D. A., Allen, J. E., Ma, Q., Herman, D. J., Tsai, W.-W., Lauhon, L. J. & Stupp, S. I. A synergistic assembly of nanoscale lamellar photoconductor hybrids. *Nat. Mater.* **8**, 68–75 (2009).
38 Tanaka, N., Okazawa, A., Sugahara, A. & Kojima, N. Development of a photoresponsive organic-inorganic hybrid magnet: layered cobalt hydroxides intercalated with spyropyran anions. *Bull. Chem. Soc. Jpn* **88**, 1150–1155 (2015).
39 Okamoto, H., Sugiyama, Y., Nakanishi, K., Ohta, T., Mitsuoka, T. & Nakano, H. Surface modification of layered polysilane with *n*-alkylamines, α,ω-diaminoalkanes, and ω-aminocarboxylic acids. *Chem. Mater.* **27**, 1292–1298 (2015).
40 Takagi, K., Shichi, T., Usami, H. & Sawaki, Y. Controlled photocycloaddition of unsaturated carboxylates intercalated in hydrotalcite clay interlayers. *J. Am. Chem. Soc.* **115**, 4339–4344 (1993).
41 Ogata, S., Tasaka, Y., Tagaya, H., Kadokawa, J. & Chiba, K. Preparation of new fibrous layered compounds by the reaction of zinc hydroxide with organic compounds. *Chem. Lett.* **27**, 237–238 (1998).
42 Oaki, Y., Ohno, H. & Kato, T. Nanosegragated composites of an imidazolium salt and a layered inorganic compound: organization of both anions and cations interlayer space. *Nanoscale* **2**, 2362–2365 (2010).
43 Takahashi, N., Hata, H. & Kuroda, K. Anion exchange layered silicates modified with ionic liquids on the interlayer surface. *Chem. Mater.* **22**, 3340–3348 (2010).
44 Maluangnont, T., Lerner, M. M. & Gotoh, K. Synthesis ternary and quaternary graphite intercalation compounds containing alkali metal cations and dications. *Inorg. Chem.* **50**, 11676–11682 (2011).
45 Osada, M., Yoguchi, S., Itose, M., Li, B.-W., Ebina, Y., Fukuda, K., Kotani, Y., Ono, K., Ueda, S. & Sasaki, T. Controlled doping of semiconducting titania nanosheets for tailored spinelectronic materials. *Nanoscale* **6**, 14227–14236 (2014).
46 Matsui, H., Oaki, Y. & Imai, H. Tunable photochemical properties of a covalently anchored and spatially confined organic polymer in a layered compound. *Nanoscale* **8**, 11076–11083 (2016).
47 Lin, Z., Rozier, P., Duployer, B., Taberna, P.-L., Anasori, B., Gogotsi, Y. & Simon, P. Electrochemical *in-situ* X-ray diffraction studies $Ti_3C_2T_x$ MXene in ionic liquid electrolyte. *Electrochem. Commun.* **72**, 50–53 (2016).
48 Gerstel, P., Lipowsky, P., Durupthy, O., Hoffmann, R. C., Bellina, P., Bill, J. & Aldinger, F. Deposition of zinc oxide and layered basic zinc salts from aqueous solutions containing amino acids and dipeptides. *J. Ceram. Soc. Jpn* **114**, 911–917 (2006).
49 Hosono, E., Mitsui, Y. & Zhou, H.-S. Metal-free organic dye sensitized solar cell based on perpendicular nanosheet thick films with high conversion efficiency. *Dalton Trans.* **40**, 5439–5441 (2008).
50 Lee, J. H., Du, Y. & O'Hare, D. Growth of oriented thin films of intercalated α-cobalt hydroxide on functionalized Au and Si substrates. *Chem. Mater.* **21**, 963–968 (2009).
51 Herman, D. J., Goldberger, J. E., Chao, S., Martin, D. T. & Stupp, S. I. Orienting periodic organic-inorganic nanoscale domains through one-step electrodepostion. *ACS Nano* **5**, 565–573 (2011).
52 Manna, M. K., Pandey, S. K., Maity, I., Mukherjee, S. & Das, A. K. Electrodeposited lamellar photoconductor nanohybrids driven by peptide self-assembly. *ChemPlusChem.* **80**, 583–590 (2015).
53 Kimitsuka, Y., Hosono, E., Ueno, S., Zhou, H.-S. & Fujihara, S. Fabrication of porous cubic architecture of ZnO using Zn-terephthalate MOFs with characteristic mictrostructures. *Inorg. Chem.* **52**, 14028–14033 (2013).
54 Ueno, N., Dwijaya, B., Uchida, Y., Egashira, Y. & Nishiyama, N. Synthesis of mesoporous ZnO, AZO, and BZO transparent conducting films using noionic triblock copolymer as template. *Mater. Lett.* **100**, 111–114 (2013).
55 Ma, C.-B., Du, B. & Wang, E. Self-crosslink method for a straightforward synthesis of poly(vinyl alcohol)-based aerogel assisted by carbon nanotube. *Adv. Funct. Mater.* **27**, 1604423 (2017).
56 Hosono, E., Fujihara, S., Honma, I. & Zhou, H.-S. The fabrication of an upright-standing zinc oxide nanosheet for use in dye-sensitized solar cells. *Adv. Mater.* **17**, 2091–2094 (2005).
57 Jayanthi, K., Nagendran, S. & Kamath, P. V. Layered double hydroxides: proposal of a one-layer cation-ordered structure model of monoclinic symmetry. *Inorg. Chem.* **54**, 8388–8395 (2015).
58 Morioka, H., Tagaya, H., Karasu, M., Kadokawa, J. & Chiba, K. Effects of zinc on the new preparation method of hydroxy double salts. *Inorg. Chem.* **38**, 4211–4216 (1999).
59 Kurmoo, M. Hard magnets based on layered cobalt hydroxide: the importance of dipolar interaction for long-range magnetic ordering. *Chem. Mater.* **11**, 3370–3378 (1999).
60 Yoon, M., Lee, J.-E., Jang, Y. J., Lim, J. W., Rani, A. & Kim, D. H. Comprehensive study on the controlled plasomon-enhanced photocatalytic activity of hybrid Au/ZnO systems mediated by thermoresposive polymer linkers. *ACS Appl. Mater. Interfaces* **7**, 21073–21081 (2015).

Supplementary Information accompanies the paper on Polymer Journal website (http://www.nature.com/pj)